Journal of Engineering Mathematics (2006) 55: 239–254
DOI 10.1007/s10665-006-9005-x

Propagation of electromagnetic waves in media undergoing complex motions

V. GLADYSHEV*, T. GLADYSHEVA and V. ZUBAREV
Physics Department, Bauman Moscow State Technical University, 5, 2-nd Baumanskaya st., Moscow 105005, Russia (E-mail: vgladyshev@mail.ru)

Received 7 June 2004; accepted in revised form 24 June 2005 / Published online: 21 April 2006

Abstract. Results of a theoretical and experimental investigation into new effects in moving-media optics are presented. An exact analytical solution is obtained for the trajectory of the wave vector of a monochromatic electromagnetic plane wave in a medium undergoing a complex motion. It is shown that the spatial dragging of the electromagnetic wave by the moving medium can be described correctly in the general case only if relativistic terms of order β^2 are taken into account. Also, in this investigation a spatial effect of the light drag was observed at a wavelength of $\lambda = 0{\cdot}63299\,\mu$m by means of an optical disk with a refractive index $n = 1{\cdot}4766$, a radius of $R_0 = 0{\cdot}06$ m rotating at a frequency of $\omega = 25$ Hz. A relative shift of the interference pattern, monitored by the time of the interference band motion across the aperture of a photodetector for the disk rotating in the opposite directions, amounted to $\Delta_{\Sigma}^{\exp} = 0{\cdot}0076 \pm 0{\cdot}0030$ of the interference bandwidth. The results of theoretical calculations of the expected interference pattern shift on the basis of the total solution of the dispersion equation in the experiment are in agreement with the experimental results. Analysis of the results obtained suggests that the detected effects determine a wide class of observed phenomena, even when the velocities of moving media are non-relativistic.

Key words: dispersion relation, electromagnetic wave, Fizeau effect

1. Introduction

Moving-medium optics, besides the classical effects of Sagnac, Fizeau and Doppler, also predicts the following phenomena: violation of Snell's law, rotation of the polarization plane of an electromagnetic wave when it is reflected from a moving boundary of two moving media, variation of the amplitude of the passing and the reflected wave, and distortion of a wave-vector trajectory of light in a medium undergoing a complex motion.

A curvature of the trajectory of an electromagnetic wave arises in the Sagnac experiment [1] when the refractive index of the medium between mirrors satisfies the condition $n > 1$, on leaving the moving frame of reference of the radiation source and detector. If the latter condition does not hold, this system is independent of the refractive index in the non-relativistic approximation, as was correctly pointed out in [2, 3].

Evidently, to describe the effect of distortion of the trajectory of an electromagnetic wave, it is necessary to use the solution of the dispersion equation of moving-medium optics for the spatial case of medium motion. Hence, the solution of the dispersion equation has been experimentally tested in special cases only.

In Sagnac-type interferometers an interference-pattern shift arises, which in the first place is attributable to cinematic motion of mirrors. A review of works on the Sagnac effect and the equations describing the electrodynamics in rotating frames can be found in [4].

* Author for correspondence

If the velocity of the medium has no tangential component ($u_{2t} = 0,\ u_{2n} \neq 0$), there is a longitudinal entrainment as found in the classic Fizeau experiment [5]. The Fizeau effect is considerably weaker than that of Sagnac. Hence, as was noticed by Arditty [6], using the rest frame of the interferometer avoids the need to take into account Fizeau and Doppler effects.

In the work of Bilger *et al.* [7], where light propagates in a rotating disk in a ring interferometer, the Fizeau effect appears, but the authors did not take into account that Snell's law is violated on the media boundary (it is a tangential break of velocity on the plane surface of the disk). Our calculation shows that the additional IP shift should be close to 20% of the general Fizeau effect.

Part of the experiments [8, 9] was devoted to attempts to estimate and measure a dispersion term in Frenel's and Lorent's formulae for fiber-optical gyroscopes. Using a low-loss fiber and very long waveguide as the beam path in ring interferometers, one can measure the rotational Fizeau drag effect. The experimental results of Vali *et al.* [10] are accurate enough to detect the presence of the dispersion term in the drag coefficient.

Some experiments [11] gave results that agree well with the solution of the electrodynamic equations for moving media with normal velocity component of the media boundary. However, these experiments constituted an experimental test of only that part of the equations which is associated with the motion of the interface, not of the medium itself. The passage of an electromagnetic wave through a medium with rotation opens up the possibility of an experimental test of the part of the solution of the dispersion equation which contains terms with u_{2t} and u_{2n}.

In the present work, the case when a light source, a receiver and a moving medium are in different frames is considered. In this case it is more effective to apply the theoretical apparatus of electrodynamics of moving media, which is based on the solution of dispersion equations complemented with boundary conditions.

The solution of the dispersion relation for the propagation of an electromagnetic wave in a medium is valid for an atomic layer with a thickness on the order of a few wavelengths of the electromagnetic radiation [12, pp. 50–51 (Russian ed.)]. For analysing each layer of the medium, the only properties available are the frequency ω_0 and the angle of incidence on the interface between two media, ϑ_0. The motion of a given layer of the medium affects the coordinates of the point at which the wave front intersects the next layer. In general, for a region of the medium in which the velocity is not constant, it is necessary to solve a dispersion equation for each neighboring local region of the medium. The complete solution is the set of local solutions for the regions in which the velocity of the medium is constant to within the physically necessary accuracy.

The propagation of electromagnetic radiation in a rotating medium is determined by the superposition of the primary wave and secondary waves appearing as a result of the interaction of the electromagnetic radiation with atoms of the moving medium. By solving a dispersion equation, it is possible to determine the radiation-wave vector in any local region of the trajectory with an allowance for the spatial distribution of the medium velocity. The validity of the solution has been repeatedly confirmed by experiment, but the complexity of such investigations allowed only certain particular cases to be studied, such as the longitudinal Fizeau effect and the normal velocity break, in which the light beam is affected by either normal or tangential components of the medium velocity.

Propagating in a rotating medium, an electromagnetic wave is affected simultaneously by both normal and tangential components of the motion. Therefore, experimental observation of the spatial effect of the light-wave entrainment confirms the validity of the total solution of the dispersion equation.

In this article a new relativistic effect is studied for a medium with permittivity ε and magnetic permeability μ undergoing a rotation ω. This effect is the curvature of the trajectory traced out by a monochromatic plane electromagnetic wave.

An exact analytical solution is obtained for the trajectory of the wave vector of a monochromatic electromagnetic plane wave in a medium with nonsimple motion (translational flow). It is shown that the spatial drag of the electromagnetic wave by the moving medium can be described correctly in the general case only if relativistic terms of order β^2 are taken into account.

Also, in this work we observe a spatial effect of the light drag at a wavelength of $\lambda = 0{\cdot}63299\,\mu$m by an optical disk with a refractive index $n = 1{\cdot}4766$, having a radius of $R_0 = 0{\cdot}06$ m and rotating at a frequency $\omega = 25$ Hz. A relative shift of the interference pattern, monitored by the time of the interference band motion across the aperture of a photodetector for the disk rotating in the opposite directions, amounted to $\Delta_\Sigma^{\exp} = 0{\cdot}0076 \pm 0{\cdot}0030$ of the interference bandwidth. The theoretical magnitude Δ_Σ is obtained while taking into account the tangential break of velocity on the plane surface of the disk; moreover, the relative error for the average value $\Delta_\Sigma^{\exp}$ is about 13%. The results of theoretical calculations of the expected interference pattern shift on the basis of the total solution of the dispersion equation in the experiment are in agreement with the experimental data.

2. Description of electromagnetic radiation in a medium undergoing a complex motion

We consider a medium in the half-space $Z < 0$ which has a permittivity ε_1 and a magnetic permeability μ_1 in a stationary frame of reference (Figure 1). There is also a medium in $Z > 0$, with permittivity ε_2 and magnetic permeability μ_2 in its stationary frame of reference. We choose a frame of reference in which the medium in $Z < 0$ is at rest, while the other medium is moving at $\boldsymbol{u}_2 = \boldsymbol{u}_{2x}\boldsymbol{e}_x + \boldsymbol{u}_{2y}\boldsymbol{e}_y + \boldsymbol{u}_{2z}\boldsymbol{e}_z$, where $\boldsymbol{e}_x, \boldsymbol{e}_y, \boldsymbol{e}_z$ are unit vectors. A monochromatic plane electromagnetic wave of frequency ω_0 is incident from the first medium on the surface of the tangential discontinuity in the (X, Y)-plane. The wave vector of the wave, $\boldsymbol{k}_0$, is in the (X, Z)-plane and makes an angle ϑ_0 with the Z-axis. According to the requirement that the phases of the incident, refracted, and reflected waves be equal at the interface, the tangential invariant corresponds to $I_t = k_{0x} = k_{1x} = k_{2x}$. The invariant $I_1 = -\omega_0 = -\omega_1 = -\omega_2$ corresponds to equality of the frequencies, due to the zero normal component of the velocity of the interface. Ignoring absorption and dispersion of the moving medium, we have, for this system, the following coordinate solution for the dispersion relation [13] of the refracted wave:

$$k_{2z} = \frac{\omega_0}{c}\left[-\kappa_2\gamma_2^2\beta_{2z}\xi_2\eta_2 + \left(\eta_2\cos^2\vartheta_0 + \kappa_2\gamma_2^2\xi_2^2\eta_2^2\right)^{1/2}\right], \tag{1}$$

where

$$\xi_2 = 1 - \beta_{2x}\sin\vartheta_0, \quad \eta_2^{-1} = 1 - \kappa_2\gamma_2^2\beta_{2z}^2,$$
$$\kappa_2 = \varepsilon_2\mu_2 - 1, \quad \beta_{2x} = \frac{u_{2x}}{c}, \quad \beta_{2z} = \frac{u_{2z}}{c},$$
$$\gamma_2^{-2} = 1 - \left(\beta_{2x}^2 + \beta_{2z}^2\right), \quad \beta_2^2 = \beta_{2x}^2 + \beta_{2z}^2.$$

For a given law of rotation centered at the point $x = 0$, $z = R_0$, the tangential and normal components of u_2 correspond to

$$u_{2x} = \omega(R_0 - z), \quad u_{2z} = \omega x, \tag{2}$$

where ω is the angular velocity.

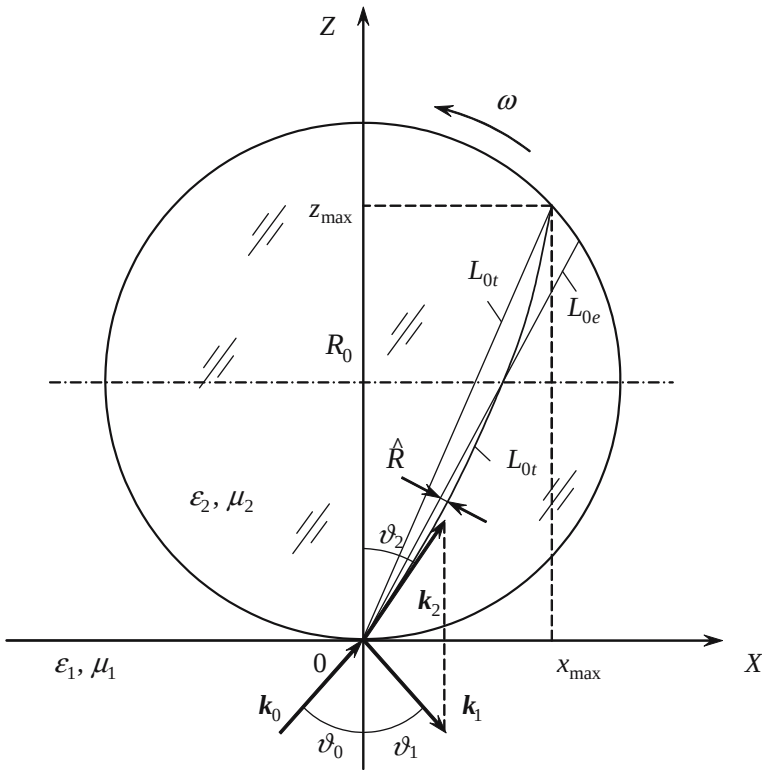

Figure 1. By virtue of the spatial effect of electromagnetic-wave dragging by a rotating medium the wave, the vector trajectory differs from a straight line.

The angle through which the electromagnetic wave is refracted, ϑ_2, is found from the relation $\tan\vartheta_2(x=0, z=0) = k_{2x}/k_{2z}$, where $k_{2x} = (\omega_0/c)\sin\vartheta_0$. We impose a boundary on the trajectory of the electromagnetic wave in the second medium: a surface of radius R_0. We require $R_0 >> \lambda_0$, where $k_0 = 2\pi/\lambda_0$ and λ_0 is a wavelength.

The trajectory lies in the (X, Z)-plane. The implicit equation

$$z = \int_0^{x_{max}(x,z)} \frac{k_{2z}}{k_{2x}}\,\mathrm{d}x \tag{3}$$

corresponds to this trajectory. Here

$$x_{max}(x, z) = \tfrac{1}{2}\sin 2\vartheta_2 \left[R_0 - \hat{k}\tan\vartheta_2 + \left(R_0^2 - 2R_0\hat{k}\tan\vartheta_2 - \hat{k}^2 \right)^{1/2} \right], \tag{4}$$

with

$$\hat{k}(x, z) = x - z\tan\vartheta_2(x, z),$$

is the coordinate of the expected intersection of the trajectory of the electromagnetic wave with the cylindrical surface. This coordinate is drifting with x, z.

Since there is no explicit general solution of (3), it is preferable, for reasons of accuracy, to use the expression $\tan\vartheta_2(x, z)$ for numerical estimates of the curvature of the trajectory. The geometric length of the trajectory of the electromagnetic wave in the rotating medium is then described by the equation

$$L_{\mathrm{t}} = \int_0^{x_{\max}(x,z)} \sqrt{1 + c\tan^2 \vartheta_2 (x, z)}\,\mathrm{d}x. \tag{5}$$

Using the expression for the geometric length of a rectilinear trajectory to the point with coordinate $z_{\max}$, *i.e.*, $L_{0\mathrm{t}} = \sqrt{2R_0 z_{\max}}$, we find the equivalent difference in path lengths for waves that have traversed the path from the point (0,0) to the point $(x_{\max}, z_{\max})$ with $\omega = 0$ and $\omega \neq 0$, respectively:

$$\mathrm{d}L_{\mathrm{cr}} = n_2 (L_{\mathrm{t}} - L_{0\mathrm{t}}). \tag{6}$$

Since the refractive index, $n_2 = \sqrt{\varepsilon_2 \mu_2}$, is not a function of the velocity of the medium, the path difference due to the longitudinal Fizeau effect clearly does not enter $\mathrm{d}L_{\mathrm{cr}}$. Working from the relation for the propagation velocity of an electromagnetic wave in the medium, $c' = -I_1 \cos \vartheta_2 / k_{2z}$, we can write down an equation for the equivalent length of the trajectory:

$$L_{\mathrm{e}} = \int_0^{x_{\max}(x,z)} \frac{k_{2z}}{(-I_1) \sin 2\vartheta_2 (x, z)}\,\mathrm{d}x. \tag{7}$$

Experimentally, one could measure the accumulated difference between the path lengths traversed by two electromagnetic waves which are incident on the interface between two media at an angle ϑ_0. One of these waves would be propagating in a medium with $\omega = 0$, and the other in a medium with $\omega \neq 0$. This accumulated path difference corresponds to

$$\mathrm{d}L_{\mathrm{e}} = L_{\mathrm{e}} - L_{0\mathrm{e}}. \tag{8}$$

The accumulated path differences due to the traverse and longitudinal entertainment effects are, respectively,

$$\mathrm{d}L_{\mathrm{t}} = n_2 (L_{\mathrm{t}} - L_0), \tag{9}$$

$$\mathrm{d}L_{\mathrm{l}} = L_{\mathrm{e}} - n_2 L_{\mathrm{t}}. \tag{10}$$

Equations (5–10) determine the physical and geometric characteristics of the transformation of an electromagnetic wave in a frame of reference with rotation.

We turn now to the results of some numerical calculations and some implications. The basic result of the calculations is to confirm that there are curvilinear propagation trajectories for electromagnetic waves in a medium with $\omega \neq 0$, as follows from Equations (1) and (2). This effect has a clear physical explanation, based on the circumstance that only one component of the wave vector, $\boldsymbol{k}_2$, changes in a moving medium. Since the equations of electrodynamics are written in an inertial frame of reference, there is a change in $\vartheta_2 = \arctan\left(k_{2x} / k_{2z}(u_2)\right)$ in each local region of the trajectory. In order words, secondary electromagnetic waves change direction in each local region of the trajectory because of a change in the projection of the velocity of the atoms of the medium onto the wave vector of the excitation wave. As a result, there is a drift of the phase velocity, and there is curvature of the trajectory representing the superposition of all waves.

Interestingly, the wave trajectories with $\omega = 0$ and $\omega \neq 0$ intersect on the straight line $z = R_0$ for arbitrary ϑ_0. Numerical values for the transverse and longitudinal entrainment effects are shown for comparison in Figure 2 in plots *vs.* ϑ_0 for the following parameter values: $k_0 = 10^{-7}\mathrm{m}^{-1}$, $n_2 = 1{\cdot}5$, $R_0 = 0{\cdot}1\,\mathrm{m}$, $\omega = 10^4\,\mathrm{rad/s}$. From the shape of the curves for $\mathrm{d}L_t$ and $\mathrm{d}L_l$ we conclude that there is a competition between effects for increasing values of ϑ_0. In the integration, the size of the local region corresponded to $\approx 10^{-5}\,\mathrm{m}$; a reduction of this value had essentially no effect on the calculated results.

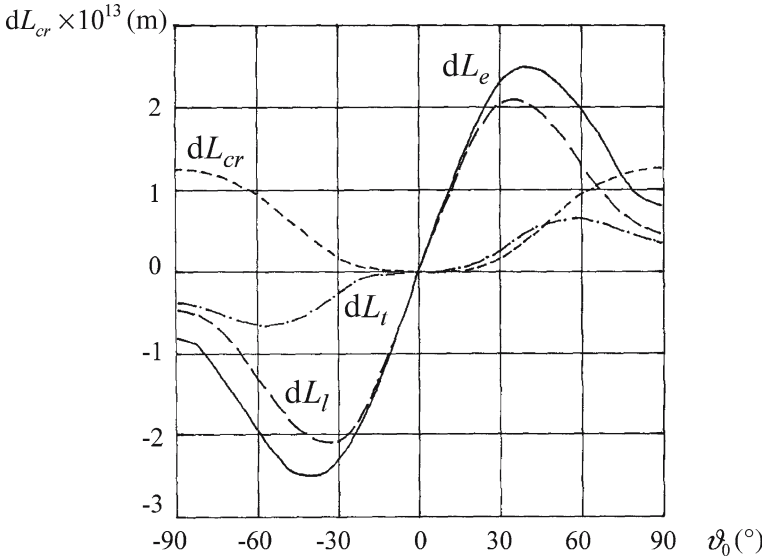

Figure 2. The dependences of the equivalent path difference dL_e, the longitudinal component of the path difference dL_t, the transverse component of the path difference dL_l with light dragging effect for two EM waves, one of which propagates in a medium with $\omega = 0$, and another with $\omega \neq 0$, on the incident angle ϑ_0 onto a boundary of two media with account of the shift of an EM radiation exit point on the surface of an optical disk. The dependence of the equivalent path difference due to bending of a trajectory without shift of an EM radiation exit point is presented as $dL_{cr}(\vartheta_0)$.

Calculations of the shortest distance, $\hat{R}$, from the curvilinear trajectory, when $\omega \neq 0$, to the straight line, along which the light propagates when $\omega = 0$, gives the deviation of the wave-vector trajectory.

As the optical path length varies with different incident angles ϑ_0, we introduce the normalized path length, which is equal to the ratio of the current path length, l_i, at the i-th point of the trajectory and the full trajectory length $\hat{J} = l_i / L_e$.

The calculation for $\hat{R}$ was made for each current point of the wave-vector trajectory with coordinates (x, z) according to the equation

$$\hat{R}(x, z) = x \cos \vartheta_2^0 - z(x) \sin \vartheta_2^0, \tag{11}$$

where ϑ_2^0 is the refractive angle for $\omega = 0$.

With Equation (3) taken into account, Equation (11) can be rewritten in terms of an integral equation:

$$\hat{R}(x, z) = x \cos \vartheta_2^0 - \sin \vartheta_2^0 \int_0^{x_{\max}(x,z)} \frac{k_{2z}(x, z)}{k_{2x}} \, dx. \tag{12}$$

The solution of the integral equation is shown in Figure 3.

As can be seen from Figure 3, the magnitude of $\hat{R}$ increases from $\hat{R} = 0$ (when $\vartheta_2^0 = 0$) to $\hat{R} \approx 10^{-7}$ m (when $\vartheta_2^0 = 90°$). The dependence $\hat{R}(\hat{J}, \vartheta_0)$ is presented in absolute values, so the dependence is divided into two parts: before intersection with the straight trajectory, where $\hat{R} > 0$, and after the intersection, when $\hat{R} < 0$.

It follows from Figure 2 that, for the assumed value of ω and $\vartheta_0 \approx 45°$, the accumulated pass difference is on the order of λ_0 for a single passage through a medium. This quantity increases linearly upon multiple rereflection at a cylindrical surface of radius R_0, which forms a symmetric nonconfocal resonator. There is accordingly a large margin in terms of accuracy

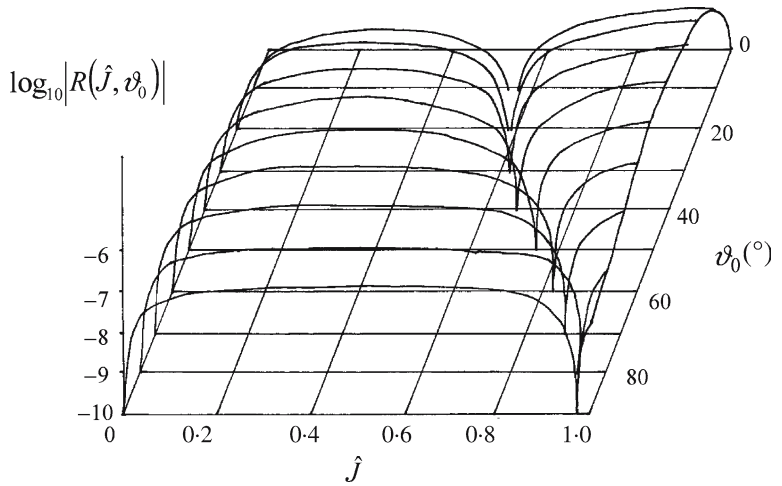

Figure 3. The dependence of the shortest distance $\hat{R}$ from the trajectory of the electromagnetic-wave vector to the straight line, along which light propagates, when $\omega = 0$, and from the incident angle ϑ_0 and normalized path length $\hat{J}$ is shown.

for studying the relativistic curvature of the propagation trajectory of a light beam in a laser-interference experiment.

3. Propagation of a monochromatic electromagnetic plane wave in a medium with translational flow

Let us consider an inertial system in which a medium with dielectric permittivity ε_1 and magnetic permittivity μ_1 is at rest in a half-space $Z < 0$, and a medium with ε_2, μ_2, measured in its own frame of reference, moving at a velocity $\boldsymbol{u}_2(x, z) = (\beta_{2x}, \beta_{2z})$ in a half-space $Z > 0$. The tangential velocity is discontinuous on the boundary of the two media. We assume that the velocity field is invariable in the direction of the axis Y.

The expression for k_{2z} imposes restrictions on its dependence on $\boldsymbol{\beta}_2(x, z)$ regarding the existence of analytical solutions of the equation for the wave-vector trajectory in the medium.

Using the dependence (1), when a solution $z = f(x)$ is sought, we obtain an implicit integral equation $z = \int_0^{x_{\max}(x,z)} f(x, z)\,\mathrm{d}x$, which, in general, does not have an analytical solution [14]. Even so, there is a case allowing an analytical solution, namely when the spatial character of the dragging effect for light appears more naturally.

Let us consider a dependence of the velocity $\boldsymbol{u}_2$ on the coordinates x, z, as follows:

$$\beta^2 = \frac{\omega^2}{c^2}(R_0 - z)^2 + \frac{\omega^2}{c^2}x^2, \tag{13}$$

which corresponds to a rotation relative to the center $(0, R_0)$ with angular velocity ω. The dependence defines the parameters $u_{2x} = \omega(R_0 - z), u_{2z} = \omega x$ as functions of the independent coordinates. Use of the relation (13), with both components taken into account, requires the numerical methods described in [15] since analytical methods result in increasing truncation errors that exceed the investigated effect.

On the other hand, the spatial character of light dragging – the curvature of the wave vector trajectory – is influenced by the tangential component of the velocity of the moving medium. Therefore, the most interesting case to study is that of spatial dragging by a moving medium.

Let us consider the case involving only a tangential component of the moving medium, β_{2x}, but with $\beta_{2z}=0$. This corresponds to the law of drift flow with a velocity that is linearly dependent on the distance from the boundary. Then, for the refractive angle ϑ_2, we can write

$$\tan^2\vartheta_2(z)=\left(\frac{k_{2x}}{k_{2z}}\right)^2=\frac{\hat{\alpha}^2\left(1-\beta_x^2(z)\right)}{\hat{\gamma}^2\left(1-\beta_x^2(z)\right)+\left(n_2^2-1\right)\left(1-\hat{\alpha}\beta_x(z)\right)^2}, \tag{14}$$

where $\hat{\alpha}=\sin\vartheta_0$, $\hat{\gamma}=\cos\vartheta_0$, $n_2=\sqrt{\varepsilon_2\mu_2}$, $\beta_x(z)=u_{2x}(z)/c$.

The wave vector, $k_0=2\pi/\lambda_0$, of an incident electromagnetic wave obeys the relation $k_0>>1/R_0$. This allows us to use solutions of a dispersion equation for a plane electromagnetic wave, having a tangential velocity discontinuity on the boundary between two media for each local field in a medium.

It is more interesting for us to study the equation, describing the trajectory of $\boldsymbol{k}_2$, based on the following analytical dependence $x=f(z)$:

$$x=\int_0^z\tan\vartheta_2(z)\mathrm{d}z. \tag{15}$$

A peculiarity of the obtained expression is that the limits can be given arbitrarily. For example, we do not have exact information about the point of intersection of the trajectory and the given cylindrical surface with radius R_0. Therefore, the integral contains a varying upper boundary. Also, we notice that the expression for the refractive angle is approximate and contains quadratic terms; this has a principal value when the spatial dragging effect by a moving medium is studied.

We will seek the solution of Equation (4) for a general case. For this, we will substitute it in (14) and make a change of the variable β_x. Then, after transformations, we will get [16]:

$$x=\tau\int_{\beta_1}^{\beta_2}\frac{(\beta_x-1)\,\mathrm{d}\beta_x}{\sqrt{G^4(\beta_x)}}, \tag{16}$$

where

$$\tau=\frac{c}{\omega}\frac{\hat{\alpha}}{\sqrt{1-n_2^2\hat{\alpha}^2}},\quad G^4(\beta_x)=(a_1-\beta_x)(a_2-\beta_x)(\beta_x-a_3)(\beta_x-a_4),$$

$$\beta_{x1,2}=\frac{\alpha\left(1-n_2^2\right)\pm\hat{\gamma}^2n_2}{1-n_2^2\alpha^2},\quad a_1=\beta_{x1},\quad a_2=-a_3=1,\quad a_4=\beta_{x2}.$$

The expression contains the square root of a polynomial of the fourth degree, and we can show that (16) can be presented as a combination of elliptic integrals. The integration limits are defined by the expression $\beta_1=\beta_{2x}(z_1)$, $\beta_2=\beta_{2x}(z_2)$ for the initial and final coordinates of the wave-vector trajectory. Let us introduce the expression

$$J_s=\int\frac{\mathrm{d}\beta_x}{(\beta_x-1)^s\sqrt{G^4(\beta_x)}}. \tag{17}$$

Then, for the coordinate x, it can be written

$$x=\tau\left(J_{-2}-2J_{-1}\right)\Big|_{\beta_1}^{\beta_2} \tag{18}$$

In order that J_{-2} can be reduced to tabulated integrals, it is necessary to increase its order. Let us decompose $G^4(\beta_x)$ in terms of powers of (β_x-1)

$$G^4(\beta_x)=b_0(\beta_x-1)^4+b_1(\beta_x-1)^3+b_2(\beta_x-1)^2+b_3(\beta_x-1)+b_4,$$

where

$$b_0 = 1, \quad b_1 = 4 - (\beta_{x1} + \beta_{x2}), \quad b_2 = 5 + \beta_{x1}\beta_{x2} - 3(\beta_{x1} + \beta_{x2}),$$
$$b_3 = 2(1 + \beta_{x1}\beta_{x2} - (\beta_{x1} + \beta_{x2})), \quad b_4 = 0.$$

By integrating the first derivative of the product

$$\sqrt{G^4(\beta_x)}\,(\beta_x - 1)^{-s},$$

we will obtain a recurrence formula, permitting to decrease the order of an elliptic integral

$$b_0(2-s)J_{s-3} + \frac{b_1}{2}(3-2s)J_{s-2} + b_2(1-s)J_{s-1} + \frac{b_3}{2}(1-2s)J_s - b_4 s J_{s+1} = \sqrt{G^4(\beta_x)}\,(\beta_x - 1)^{-s}, \quad s = 1, 2, 3, \ldots \tag{19}$$

By using (19) with $s = 1$ and taking into account that $b_4 = 0$, we will get the following expression for J_{-2}:

$$J_{-2} = \frac{1}{2b_0}\left(\frac{2\sqrt{G^4(\beta_x)}}{\beta_x - 1} - b_1 J_{-1} + b_3 J_1\right). \tag{20}$$

After substitution of (20) in (18), the expression for x will become

$$x = \frac{\tau}{2b_0}\left(\frac{2\sqrt{G^4(\beta_x)}}{\beta_x - 1} + b_3 J_1 + (4b_0 - b_1)J_{-1}\right)\Bigg|_{\beta_1}^{\beta_2}. \tag{21}$$

It should be noted that the inequalities

$$a_1 > a_2 \geq \beta_x > a_3 > a_4$$

are fulfilled, and we introduce

$$I_1 = \int_c^{\beta_x} \frac{\beta_x \mathrm{d}\beta_x}{\sqrt{G^4(\beta_x)}}, \quad I_2 = \int_c^{\beta_x} \frac{\mathrm{d}\beta_x}{\sqrt{G^4(\beta_x)}}, \quad I_3 = -J_1\,|_c^{\beta_x}.$$

Then, Equation (10) can be expressed via tabulated integrals

$$x = \frac{\tau}{2b_0}\left(\frac{2\sqrt{G^4(\beta_x)}}{\beta_x - 1} - b_3 I_3 + (4b_0 - b_1)(I_1 - I_2)\right)\Bigg|_{\beta_1}^{\beta_2}, \tag{22}$$

$$I_1 = 2g[(a_3 - a_4)\Pi(\varphi, \bar{n}_1, k) + a_4 F(\varphi, k)],$$

$$I_2 = 2gF(\varphi, k),$$

$$I_3 = 2gq[(a_3 - a_4)\Pi(\varphi, \bar{n}_2, k) + (1 - a_3)F(\varphi, k)],$$

$$g = \frac{1}{\sqrt{(a_1 - a_3)(a_2 - a_4)}}, \quad q = \frac{1}{(1 - a_3)(1 - a_4)},$$

where $F(\varphi, k)$ and $\Pi(\varphi, \bar{n}_i, k)$ are normal elliptic integrals of the first and third kind, to which the characteristics $\bar{n}_1$, $\bar{n}_2$, amplitude φ and modulus k are related as follows:

$$\bar{n}_1 = \frac{a_2 - a_3}{a_2 - a_4}, \quad \bar{n}_2 = \frac{(a_2 - a_3)(1 - a_4)}{(a_2 - a_4)(1 - a_3)},$$

$$\varphi = \arcsin\sqrt{\frac{(a_2-a_4)(\beta_x-a_3)}{(a_2-a_3)(\beta_x-a_4)}}, \quad k = \sqrt{\frac{(a_2-a_3)(a_1-a_4)}{(a_1-a_3)(a_2-a_4)}}.$$

By substituting the coefficients a_1, a_2, a_3, a_4, we finally have

$$x = \tau\left(\lambda\left[(c_1\Pi(\varphi,\bar{n}_2,k) - c_2\Pi(\varphi,\bar{n}_1,k) - c_3F(\varphi,k)\right] - \frac{\sqrt{G^4(\beta_x)}}{1-\beta_x}\right)\Bigg|_{\beta_1}^{\beta_2}, \tag{23}$$

where $c_1 = (1+\beta_{x2})(1-\beta_{x1})$, $c_2 = (1+\beta_{x2})(\beta_{x2}+\beta_{x1})$,
$c_3 = 2(1-\beta_{x1}) + (1-\beta_{x2})(\beta_{x2}+\beta_{x1})$, $\lambda^{-2} = (1+\beta_{x1})(1-\beta_{x2})$.

Comparison of the calculated results using the formula (23) with elliptic-integral tables [17] and direct calculations with formulae (15) shows that the accuracy of the analytical calculations depends on the tabular step and interpolations are needed. Hence, up to this effect, the obtained expression is exact.

We can notice that $\bar{n}_2 = 1$ for any a_4. In this case $\Pi(\varphi, \bar{n}_2, k)$ can be expressed via elliptic integrals of the first and second kind:

$$\Pi(\varphi,\bar{n}_2=1,k) = F(\varphi,k) - sec^2\alpha\,(E(\varphi,k) - \tan\varphi\Delta\varphi),$$
$$\Delta\varphi = \sqrt{1-k^2\sin^2\varphi}, \quad k = \sin\alpha.$$

Using these expressions reduces the interpolation error due to a more accurate computation of the tables for $F(\varphi,k)$ and $E(\varphi,k)$.

4. Experimental test of the solution of the dispersion equation for the propagation of an electromagnetic wave in rotating optical media

Propagating in a rotating optical disk, the electromagnetic wave is simultaneously affected by normal and tangential components of the velocity of the motion. Experimental observation of the spatial effect of the light-wave drag validates the solution of the dispersion equation in the general case. For achieving this goal a double-beam two-pass disk interferometer was designed and built with inputting beams into the flat surface of an optical disk (Figure 4).

In this scheme, the light beam from laser L incident on a beam divider BD was split into two beams. These beams entered the optical disk OD (one of these after reflecting on the mirror M) to be reflected from the flat mirror surfaces of the OD. The exit beams reflected from the prism AP changed paths, passed through the optical disk in the reverse direction, and entered the divider again. Mixed on the divider mirror, the beams passed through an optical system OS to display the interference pattern on a screen S. The light intensity was measured by photodetector PD.

The signal from the photodetector passed through a resistor system into an oscillograph. A digital Kodak DC240 camera with high resolution and a recording element recorded the oscillograms (25 tests for each combination of rotation direction and an adjustment) and was then processed and analyzed on a personal computer. Compensating difference features of the scheme provided high protection against mechanical disturbances.

The interferometer was tuned to interference fringes of equal thickness and determined the shift of the light-interference pattern using the time signal from the photodetector, when the optical disk OD rotates. The direction of the interference-pattern (IP) shift in the plane of analysis of the IP depends on the rotation direction.

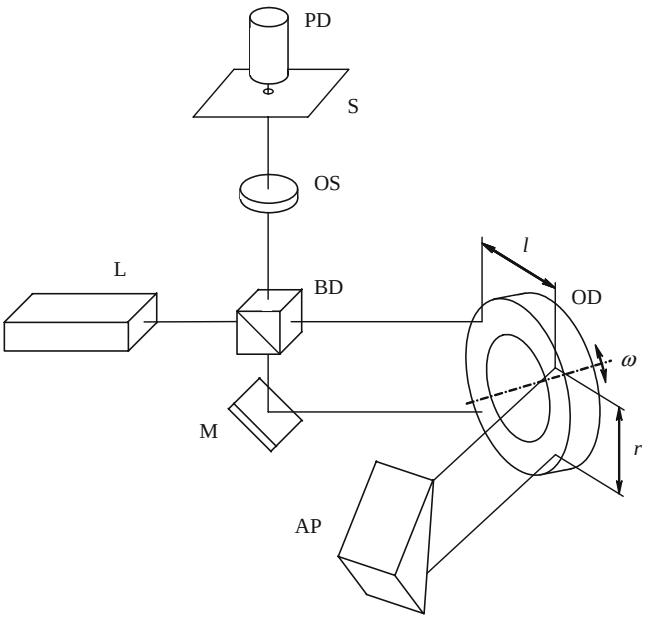

Figure 4. The optical scheme of the interferometer with a rotating optical disk. The scheme realizes the method of IP shift detection by measuring the time of IP moving on the photodetector.

This method of picking out the time signal is preferred to the method of measuring the variations in intensity, because the time of IP motion is measured by equipment that has a higher relative resolution and parameter stability.

After adjusting the OD, the beam spots moved in ellipses on a screen upon slowly rotating the OD. The ellipticity of the curves is explained by the photoelastic effect. After adjusting the optical system, checking the stability of the motor while operating, and achieving a stable IP, the experiment was carried out. When a light beam propagates in a rotating optical disk, the vector of linear velocity changes its direction in space from point to point; hence the longitudinal effect of changing light and the transverse deviation of the beam trajectory should be observed.

To estimate the light-dragging effect, let us consider the solution of the dispersion equation in the plane XOZ and in the plane of incident and reflected beams. In our experiment a beam is incident out of a medium with $n_0 = 1$ onto the flat surface of the optical disk with a refractive index n_2 under an angle ϑ_0 (Figure 5). As the longitudinal light-dragging effect is determined with the longitudinal component of the linear velocity of motion, we can consider Equation (1) for $\beta_{2x} = 0$ and $\vartheta_0 = 0$; hence

$$k_{2z} = \frac{\omega_0}{c} \frac{-\kappa_2 \gamma_2^2 \beta_{2z} \pm \sqrt{1 + \kappa_2 \gamma_2^2 \left(1 - \beta_{2z}^2\right)}}{1 - \kappa_2 \gamma_2^2 \beta_{2z}^2}, \tag{24}$$

Considering $\beta_{2z} >> \beta_{2z}^2$, we obtain an expression for the phase light velocity in a rotating medium

$$c' = \frac{\omega_0}{\sqrt{k_{2x}^2 + k_{2z}^2}} \cong \frac{c}{n_2} \pm u_2 \left(1 - \frac{1}{n_2^2}\right). \tag{25}$$

The orientation of $\boldsymbol{k}_2$ and $\boldsymbol{u}_2$ varies along the beam trajectory; therefore for a spatial case we should use the projection of the medium velocity vector onto the wave vector instead of $\boldsymbol{u}_2$ in (25):

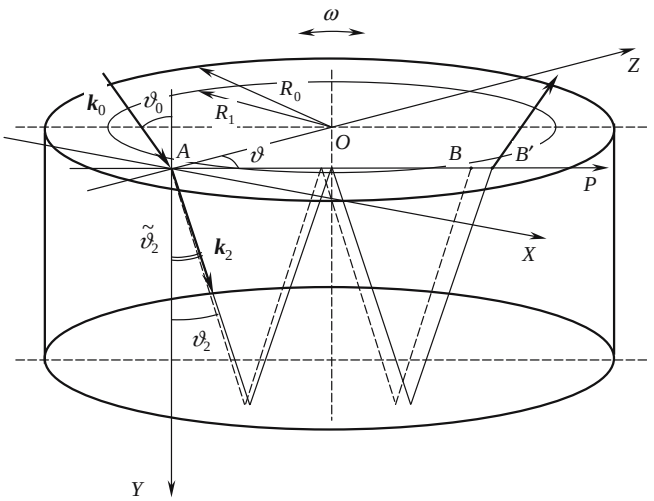

Figure 5. The optical disk OD. The upper surface of OD has the partial reflective layer with radius R_1, the lower has full reflective cover. Due to the deviation from Snell's law, the exit point of beam B for the stationary disk shifts from its position to point B′ for the rotating disk.

$$\boldsymbol{u}_{2k} = u_{2z}\cos\vartheta\sin\vartheta_2 + u_{2x}\sin\vartheta\sin\vartheta_2, \tag{26}$$

with $u_{2x} = \omega(R-z)$, $u_{2z} = \omega x$, $R = OA$ and ϑ_2 being the angle of refraction. Further we will take into account that phase accumulation due to trajectory curvature in the plane X, Z is not large in comparison with the longitudinal effect [15].

We can now show that $\boldsymbol{u}_{2k} = \omega R\sin\vartheta\sin\vartheta_2$ at any point of the trajectory. When beams pass through the rotating OD a single time, the IP shift is equal to

$$\Delta_0 = \frac{\tilde{n}}{\lambda_0}(t_2 - t_1), \tag{27}$$

$$t_1 = \frac{d}{\cos\vartheta_2\left(\frac{c}{n_2} + \left(1 - \frac{1}{n_2^2}\right)\omega R\sin\vartheta\sin\vartheta_2\right)}, \quad t_2 = \frac{n_2 d}{c\cos\vartheta_2}, \tag{28}$$

where λ_0 denotes the wave length of light; t_1, t_2 are the times of passing through the rotating and static OD, respectively; ω is the OD angular velocity and d the OD thickness.

After substituting t_1, t_2 in (27), we obtain in the limit $\omega R << c$:

$$\Delta_0 = \frac{\kappa_2\omega r\sqrt{R^2 - r^2}}{\lambda_0 c}. \tag{29}$$

Here r is the distance between the projection of the beam path in OD and the center of rotation, $r = OA\sin\vartheta$ (Figure 5). By giving the value of R, we can find the optimal value r for which Δ_0 will be maximal. From the equation $\frac{\partial\Delta_0}{\partial r} = 0$ we obtain that the optimal value is equal to $r = R/\sqrt{2}$.

The determined value of the IP shift Δ in the interferometer should be equal to $32\Delta_0$. First, the disk-edge surfaces are mirror-coated, thus doubling the optical path. After reflecting from a prismatic reflector the beams repeatedly pass through OD, which also increases the resulting IP shift by a factor of 2. In the scheme we use two opposite beams and two directions of rotation which increases the resulting IP shift by a factor of 4. Carrying out

the experiments for two different adjustments allows an increase of the resulting IP shift by another factor of 2.

As a result of this we can write

$$\Delta = \frac{16 l u_{2n}(n_2^2 - 1)}{\lambda_0 c}, \tag{30}$$

where $l = AB'$ is the projection of beam path in OD onto the flat surface of the disk (Figure 5); further $u_{2n} = \omega r$ is the linear medium velocity along the light-beam trajectory.

In reality, the IP shift can be increased due to the refraction angle $\tilde{\vartheta}_2$ which differs from the one calculated by Snell's law, ϑ_2. As the trajectory curvature is small, we consider a beam that propagates in the plane POY (Figure 5). The projection of a wave vector on the axis P can be found from the solution of the dispersion equation, supposing $\beta_{2y} = 0$ and $\beta_{2z} >> \beta_{2z}^2$:

$$k_{2pz} = \frac{\omega_0}{c}\left(-\kappa_2 \beta_{2z} + \sqrt{\cos^2 \vartheta_0 + \kappa_2}\right), \tag{31}$$

where ϑ_0 is the angle of refraction.

The refraction angle in a moving medium is obtained from

$$\tan \tilde{\vartheta}_2 = \frac{\sin \vartheta_0}{-\kappa_2 \beta_{2z} + \sqrt{\cos^2 \vartheta_0 + \kappa_2}}. \tag{32}$$

The increase of the optical path length in OD is equal to the difference between the equivalent optical path l_e in a rotating medium and the one l_{0e} in a static medium:

$$\Delta \tilde{l}_e = l_e - l_{0e} = 4\,\mathrm{d} n_2 \left(\frac{1}{\cos \tilde{\vartheta}_2} - \frac{1}{\cos \vartheta_2}\right). \tag{33}$$

If OD is stationary, the beam traverses the path in air. The increase in the optical path length is equal to

$$\Delta l_e = \Delta \tilde{l}_e \left(1 - \frac{1}{n_2}\right). \tag{34}$$

This value determines the additional path difference of the beam, for the OD passes each time in one direction, due to a deflection by Snell's law.

The resulting value of the additional shift, due to this effect, with account taken of all passes of two beams for all directions and adjustments in our experiment, is equal to

$$\Delta_S = 16 \frac{\Delta l_e}{\lambda_0}. \tag{35}$$

Also, we can estimate the value of the additional IP shift as a result of the curvature of the beam-motion trajectory in a rotating medium. However, for our scheme the opposite beams have curved trajectories, so the resulting value of the IP shift will tend to zero.

The total shift due to the light-dragging effect and the deviation from Snell's law, is

$$\Delta_\Sigma = \Delta + \Delta_S. \tag{36}$$

The expected shift was calculated for the interferometer parameters used in our experiment:

$$\Delta = 0{\cdot}0054 \text{ bandwidth}, \Delta_S = 0{\cdot}0013 \text{ bandwidth}, \Delta_\Sigma = 0{\cdot}0067 \text{ bandwidth}. \tag{37}$$

In the experiment the gas-atomic stabilised laser LGN-302, operating in continuous mode ($\lambda_0 = 0{\cdot}632991\,\mu$m), was as a light source. The optical disk was a standard plate with a diameter of 120 mm and a thickness of 30 mm and was made of LK5-grade glass ($n_2 = 1{\cdot}4766$).

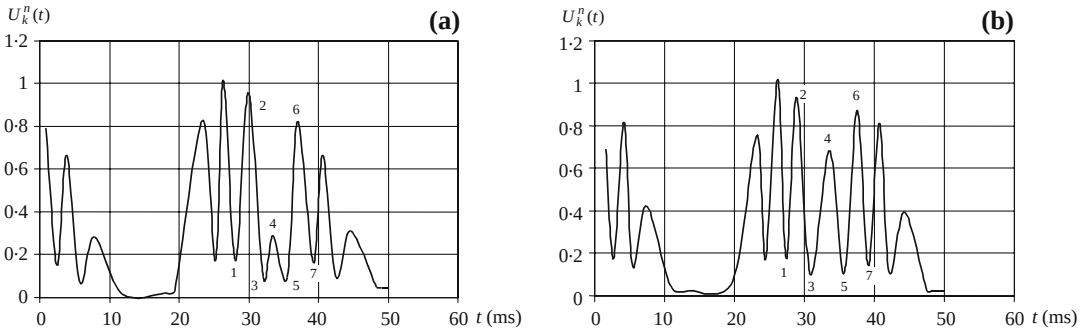

Figure 6. The dependence of the relative voltage of the photodetector PD on time when the first adjustment for the right (a) and left (b) directions of rotation is used.

One edge surface of a disk and part of another edge surface of a disk with a diameter of 80 mm were fully coated to provide for a reflection coefficient of $\rho = 0{\cdot}9$. In the experiment we used an asynchronous three-phase motor. The average rotation period is $\bar{T} = 0{\cdot}0396$ s, that is, relative to a rotation frequency of 25·26 Hz. The deviation of the rotation speed remained within $\pm 1\%$. To decrease the influence of vibrations, the optical system and the motor with OD was placed on different platforms and tables.

When we used the first adjustment and a counterclockwise direction of the motor rotation, interference fringes tended to incline to the right and were reset to the original position (Figure 6a). When the OD was slowly rotated, it was observed that three bands passed across the photodetector aperture in the forward and reverse directions. Between the motions the stopping point was observed. The photodetector was arranged so that it was between minimum and maximum of the intensity of a band in the stop position.

The basic unit of the scale used for measuring the experimental results was 1 ms so that points 1–7 could be accommodated on the oscillograph screen.

The readings t_{kj}, where k numbers the points, were taken from oscillograms. Thereupon the values were calculated, using

$$\delta t_j = (t_{5j} - t_{3j})/2, \quad j = \overline{1,\ 25}, \tag{38}$$

$$\Delta t_j = (t_{3j} - t_{2j} + t_{6j} - t_{5j})/2, \tag{39}$$

where δt_j corresponds to the time-distance values between the IP stopping point and the nearest interference band and Δt_j corresponds to the time width of the interference fringe. After this, we processed the oscillograms, using the clockwise direction of the motor rotation, in the same way (Figure 6b).

The next adjustment was carried out with interference fringes inclining to the left. Second directions of motor rotation were used also for the second adjustment. In the experiment we detected time coordinates of the t_k points, when IP moved, so it was necessary to convert them to the spatial ones. The relation between Δt and δt determines the relative position of an interference fringe in the part of the time bandwidth.

We noticed that beams on the screen moved in ellipses. The ellipse length is determined using an elliptic integral of the second kind.

We can change the values Δt and δt for the ellipse arc lengths δL and $\Delta L_{\sum}$, expressed in radians, as follows:

$$\delta L = \pi \frac{\delta t}{T}, \quad \Delta L_\Sigma = \delta L + \Delta L/2 = \pi \frac{\delta t + \Delta t}{T}, \tag{40}$$

$$\delta L = a \int_0^{\varphi_5} \sqrt{1 - \sin^2 \alpha \ \sin \varphi}\, \mathrm{d}\varphi = a\, E(\varphi_5 \backslash \alpha), \tag{41}$$

$$\Delta L_\Sigma = a \int_0^{\varphi_6} \sqrt{1 - \sin^2 \alpha \ \sin \varphi}\, \mathrm{d}\varphi = a\, E(\varphi_6 \backslash \alpha), \tag{42}$$

where $\sin^2 \alpha = 1 - b^2/a^2$, a, b are the major and minor ellipse half-axes, T the period of IP vibrations, $E(\varphi_5 \backslash \alpha), E(\varphi_6 \backslash \alpha)$ elliptic integrals of the second kind, φ the parameter of the elliptic integral and φ_5, φ_6, the parameters referring to the points 5 and 6.

Inserting the values Δt and δt, which were measured in the experiment, into Equation (37), we can get ΔL and δL_Σ. It follows from (40) to (42) that $a = 1$ since the values Δt and δt have been normalised by the period T. Then, using Equations (41) and (42), the relation b/a taken from the experiment, and tables of elliptic integrals of the second kind, we can determine φ_5 and φ_6.

The relative position of a band from point 4 is determined as

$$\Delta = \frac{\delta y}{\Delta y} = \frac{1 - \cos \varphi_5}{2(\cos \varphi_5 - \cos \varphi_6)}. \tag{43}$$

Here δy is the spatial position of a band from the point 4 and Δy is the spatial bandwidth

$$\delta y = b(1 - \cos \varphi_5), \quad \Delta y = 2b(1 - \cos \varphi_6 - \delta y).$$

For two rotation directions and two adjustments of the interfering beams, we can obtain the resulting measured value of the IP shift:

$$\Delta_\Sigma = (\Delta_1 - \Delta_2) - (\Delta_3 - \Delta_4). \tag{44}$$

We notice that calculating the IP shift is carried out for the values that are normalized with respect to a rotation period and to the interference band width. Thus, the results of the calculation do not depend on the period of the vibrations and bandwidth from one measurement to the other. For the series of the experimental data Δ_i the confidence intervals were calculated with a confidence probability of $p = 0{\cdot}9$. Then, the resulting value of the shift turned out to be equal to

$$\Delta_\Sigma^{\mathrm{Exp}} = 0{\cdot}0076 \pm 0{\cdot}0030 \text{ bandwidth} \tag{45}$$

The theoretical magnitude $\Delta_\Sigma = 0{\cdot}0067$ falls within the confidence interval (42); moreover, the relative error of the average value $\Delta_\Sigma^{\mathrm{exp}}$ is about 13%.

5. Conclusion

We have found that spatial electromagnetic-wave dragging by a rotating medium should be taken into account for non-relativistic velocities of the medium. This effect may have an impact on the results of different measurement procedures [18]. The results of theoretical calculations of the expected IP shift for the used parameters in the experiment were found to be in agreement with the experimental results of the IP shift. It should be noticed that the rotation velocity in the experiment was not high. But the spatial light-dragging effect had an influence on the IP shift.

In order to make the final conclusion that the experimental results are in agreement with relativistic predictions, it is necessary to increase the experimental accuracy. This may be

achieved by using a more stable motor with higher rotation frequency and a more sophisticated system of transforming the signal from a photodetector.

In conclusion, from an experimental point of view a study of this physical effect, namely the curvature of the propagation trajectory of a monochromatic plane electromagnetic wave in a medium with $\omega \neq 0$, involves not only a determination of the curvature and the possibility of carrying out a new experimental test of the electrodynamics of moving media, but also the construction of a new relativistic interferometer.

Acknowledgement

This work was supported by Grants Council of the President of Russian Federation (grant №̲ MD-170.2003.08).

References

1. G. Sagnac, L'ether lumineux demontre par l'effect du vent relative d'ether dans un interferometer en rotation uniforme. *C.R. Acad. Sci.* 33 (1913) 349–354.
2. A.A. Logunov and Yu.V. Chugreev, Special theory of relativity and the Sagnac effect. *Sov. Phys. Usp*. 31 (1998) 861–867.
3. C.V. Heer, Resonant frequencies of an electromagnetic cavity in an accelerated system of reference. *Phys. Rev. A*. 134 (1964) 799
4. E.J. Post, Sagnac effect. *Rev. Mod. Phys.* 39 (1967) 475–494.
5. H. d'Fizeau, Sur les hypotesis relatives a l'ether lumineux, et sur une experience qui parait demonter que le mouvement des corps change la vitesse avec laquelle la lumiere se propage dans leur interieur. *Ann. Chim. Phys.* 57 (1859) 385.
6. H.J. Arditty and H.C. Lefevre, Sagnac effect in fiber gyroscopes. *Opt. Lett.* 6 (1981) 401–403.
7. H.R. Bilger and W.K. Stowell, Light drag in a ring laser: An improved determination of the drag coefficient. *Phys. Rev. A.* 16 (1977) 313–319.
8. I. Lerche, The Fizeau effect: Theory, experiment, and Zeemen's measurements. *Am. J. Phys.* 45 (1977) 1154–1163.
9. W.R. Leeb, G. Schiffner and E. Scheiterer, Optical fiber gyroscopes: Sagnac or Fizeau effect? *Appl. Opt*. 18 (1979) 1293–1295.
10. V. Vali, R.W. Shorthill and M.F. Berg, Fresnel-Fizeau effect in a rotating optical fiber ring interferometer. *Appl. Opt.* 16 (1977) 2605–2607.
11. O.G. Zagorodnov, Ya.B. Fainberg and A.M. Egorov, Frequency multiplication by using the plasma "collapse". *JETP* 38 (1960) 7–9.
12. S. Solimeno, B. Crosignani and P. DiPorto, *Guiding, Diffraction, and Confinement of Optical Radiation*. Orlando: Academic Press. (Russian edition (1986) 664 pp.)
13. B.M. Bolotovskii and S.N. Stolyarov, Reflection of light from a moving mirror and related tasks. *Sov. Phys. Usp.* 32 (1989) 813–838.
14. V.O. Gladyshev, T.M. Gladysheva and V.Ye. Zubarev, The effect of light entrainment observed in an optical disk interferometer. *Tech. Phys. Lett.* 28 (2002) 123–125.
15. V.O. Gladyshev, Curvature of the trajectory traced out by a monochromatic plane electromagnetic wave in a medium with rotation. *JETP Lett.* 58 (1993) 569–572.
16. V.O. Gladyshev, Propagation of a monochromatic electromagnetic plane wave in a medium with nonsimple motion. *Tech. Phys.* 44 (1999) 566–569.
17. M. Abramowitz and I. Stegun, *Handbook of Mathematical Functions*. Washington: National Bureau of Standards. (1964) 1046 pp.
18. V. Gladyshev, T. Gladysheva and V. Zubarev, Description of electromagnetic radiation in complex motion media with account of the relativistic effects. In: M.C. Duffy, V.O. Gladyshev and A.N. Morozov (eds.), *Proc. of Int. Meeting Phys. Interpretations of Relativity Theory*. Moscow-Liverpool-Sunderland (2003) pp. 112–121.